Weak-Coupled Cross-Sectional Differential-Paired Lines with Bend Discontinuities for SI and EMI Performances

Yoshiki KAYANO, Masashi OHKOSHI
Department of Electrical and Electronic Engineering,
Akita University
1-1 Tegata-gakuen-machi, Akita-shi, 010-8502, Japan
Email: kayano@gipc.akita-u.ac.jp

Hiroshi INOUE
Akita Study Center,
The Open University of Japan
1-1 Tegata-gakuen-machi, Akita-shi, 010-8502, Japan
Email: inoueh@gipc.akita-u.ac.jp

Abstract—**For differential-signaling system, the ideal balance or symmetrical topology cannot be established due to bend (turnoff point) discontinuities, and hence, an imbalance component is excited. Therefore methodology and geometrical-structure for satisfying both SI and EMI performances are indispensable. In order to provide basic considerations for the realization of methods for predicting and suppressing the EM radiation from asymmetrical differential-paired lines, the imbalance component and EMI from strong and weak coupled differential-paired lines with bend discontinuities were studied experimentally and with modeling. Firstly differential-mode impedance and the mixed-mode scattering parameters are discussed, from view point of SI performance. Secondly, frequency response of electric field near a PCB are discussed, from view point of EMI. It is demonstrated that the differential-paired line with weak-coupling is suitable for improving the SI performance and suppressing the EMI. This study has successfully reported the basic characteristics of imbalance component of differential-paired lines with bend routing and demonstrates the dominant factor of imbalance component.**

Keywords—differential-signaling, differential-paired lines, differential-mode, common-mode, imbalance

I. INTRODUCTION

Differential-signalling (DS) scheme is one of the key technologies for modern electronics systems. DS techniques such as low-voltage differential-signaling (LVDS) are widely used in digital electronic devices in order to establish a high-speed digital propagation with low-electromagnetic interference (EMI) [1], [2]. In actual differential-paired lines, there are the non-ideal symmetrical topology, discontinuity of the differential-mode (DM) impedance of the differential-paired lines, and the skew and distortion of the traveling-waveform due to a bend topology. Hence, unintentional imbalance components between voltages traveling the differential paired lines deteriorate signal integrity (SI) and intensify EMI.

Many papers have demonstrated that imbalance components (common-mode: CM) in differential signals, due to a bend region and asymetrical layout, deteriorate SI and EMI performances, and then discussed suppression of imbalance component by CM choke, periodic structure and new layout for compensation [3]–[8]. So far, the taper bend discontinuities and meander delay line as equi-distance routing technique have been proposed to improve and compensate SI performance. But the papers have mainly focused on SI issue. Therefore general study for predicting and suppressing EMI as well as establishment of signal integrity over a broad band are required.

The previous studies [9]–[13] have demonstrated that the conversion parameter from DM (balance component) to CM (imbalance component), $|S_{cd21}|$, is significantly increased by the difference of the length. Frequency response of the EM radiation from an asymmetrical differential-paired lines on an infinite ground plane can be identified and quantified, using the physics-based model, which is constructed with an equivalent circuit model to calculate current distribution, and radiation model based on Hertzian dipole antenna. Although equi-distance routing is suitable for the improvement of SI issues, it is not considered for the suppression of the radiated emission. The results indicate that the $|S_{cd21}|$ is not a single evaluator for predicting the EM radiation. For mitigation of EMI problems underlying differential-paired lines, the identification of the dominant factors which generate the imbalance component should be an important issue in order to quantify the relationship between the EMI and the configurations at the design stage for practical applications. Especially, the case where the power and/or ground plane are located near differential-paired lines has trended in practical applications such as FPC and multilayered PCB. As this fact influences on coupling-strength between the differential-paired lines strongly, the development of methodology and design guidelines of geometrical-structure for satisfying both SI and EMI performances are indispensable.

This paper focuses on the cross-sectional structure for establishing SI performance and suppressing imbalance component and EMI generated by differential-paired lines with bend (turnoff point) discontinuities, which depend on strength of coupling between paired lines. To provide the basic considerations for EM radiation from practical asymmetrical differential-paired lines structure with bend routing, we newly attempt to identify and quantify the imbalance component and EMI from strong and weak coupled differential-paired lines with bend region. The main goal of this study is to clarify the characteristics and dominant radiation factor of such PCBs and to acquire basic insights for designing way for both SI and EMI performances. The PCB geometries used in the study are described in Section 2. In Section 3, differential-mode impedance and the mixed-mode scattering parameters are discussed, from view point of SI performance. In Section 4, frequency response of electric field near a PCB are discussed, from view point of EMI.

II. PCB Geometry Under Study

Bended differential-paired lines with different coupled cross-section were prepared as typical routing. The geometry and cross-sectional views of the PCBs under study for appropriate simple model for studying and getting physical-insights are illustrated in Figs. 1 and 2. The PCB has cross sectional three layers, with the upper layer for the signal trace, middle layer for the dielectric substrate and the lower layer for the reference (ground) plane. The size of the PCB structure used for the test model is l=100 mm (length), w=100 mm (width). As the focuses in this paper are on the imbalance component generated by asymmetrical topologies, the relatively wide separation s=1.0 mm is selected so that an imbalanced component due to the asymmetrical structure is the dominant fact of the EM radiation compared with that due to the waveform distortion of the output of the LVDS driver.

In order to change the coupling strength between the differential-paired lines, thickness h and relative permittivity of ε_r of dielectric substrate are changed while s=1.0 mm is constant. For the "Strong-coupling" ($h > s$) case, the FR-4 substrate with h=1.53 mm, ε_r=4.5, $\tan\delta$=0.015 is used for dielectric material, called "Strong" as shown in Fig. 2(a). For the "Weak-coupling" ($h < s$) case, the CGP-500 substrate with h=0.43 mm, ε_r=2.6 and $\tan\delta$=0.0018 is used for dielectric material, called "Weak" as shown in Fig. 2(b). Both differential-paired lines have the differential mode impedance Z_{DM}=100 Ω, by changing width of the paired lines w_t. The dominant factor of generation of imbalance component of the model under study is difference of the geometrical length between Line 1 and 2 due to the bend routing. Similar phenomenon occurs when the one trace is slightly longer than the other even if there is no bend. Nevertheless, the bend region is used in this study to model and study typical routing in practical systems.

III. Imbalance Component on Differential-Paired Lines Structure

A. Evaluation of Differential-Mode Impedance

The differential-mode impedance Z_{DM} of the differential-paired lines was measured by using a time domain reflectmetry (TDR) system (Agilent 86100A). The results of the Z_{DM} are shown in Fig. 3. The unit of the longitudinal axis is converted into impedance [Ω], after the calibration by 50 Ω at 0 ns. Region before t=0.18 ns is cable for connection, and region after t=0.18 ns is the differential-paired lines.

The Z_{DM} except bend and taper region is approximately 100 Ω. The differences of the propagation time result from the variation of effective dielectric constant. As the results, the influence of bend and taper regions in the "Weak" case is smaller than compared with that in the "Strong" case. This is one of advantage in high-speed signal transmission.

B. Evaluation of Mixed-Mode S parameter

The frequency responses of mixed-mode scattering parameters are shown in Figs. 4 and 5. The solid and broken lines show the measured results by the network analyzer with 4 ports and the calculated results by MoM, respectively. Figure 4 shows the measured frequency response of $|S_{dd21}|$, which is defined as the transmission coefficient of the differential-mode.

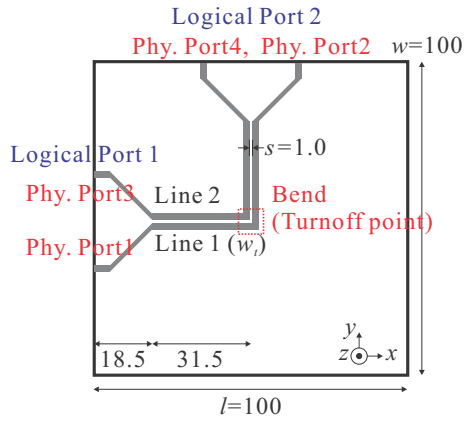

Fig. 1. Geometry of the PCBs under study (in mm).

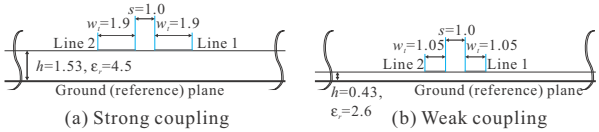

Fig. 2. Cross-sectional views (in mm).

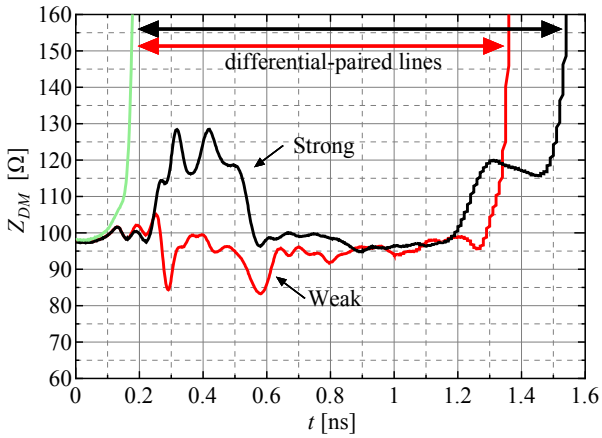

Fig. 3. Results on TDR measurement

Remarkable difference between two cases is deterioration of $|S_{dd21}|$ dut to a dielectric loss at gigahertz frequency band. Nevertheless, there is no resonance and anti-resonance due to the bend-routing.

Figure 5 shows the frequency response of $|S_{cd21}|$, which is defined as the conversion from differential-mode (balance component) to common-mode (imbalance component). The measured and calculated results are in good agreement. The "Weak" case can suppress the $|S_{cd21}|$ at lower frequency compared with the "Strong" case, because the difference of traveling path between Line 1 and 2 is relatively small due to the narrow width w_t, and the electric-field is distributed between the trace and ground plane.

In order to identify the dominant generation factor of the imbalance component, the single-end s-parameters are measured. The single-end s-parameters is related to Mixed-mode s-parameter:

$$S_{cd21} = \frac{S_{21} - S_{43} + S_{41} - S_{23}}{2}. \quad (1)$$

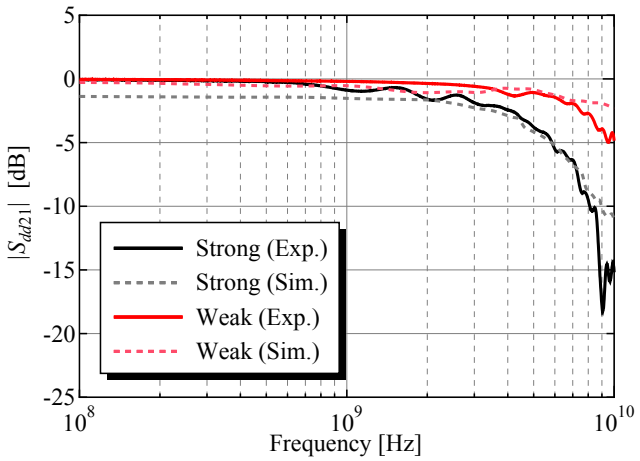

Fig. 4. Frequency response of $|S_{dd21}|$.

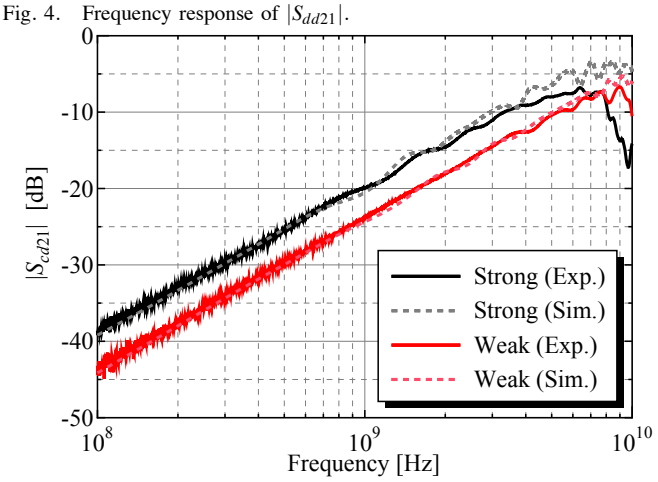

Fig. 5. Frequency response of $|S_{cd21}|$.

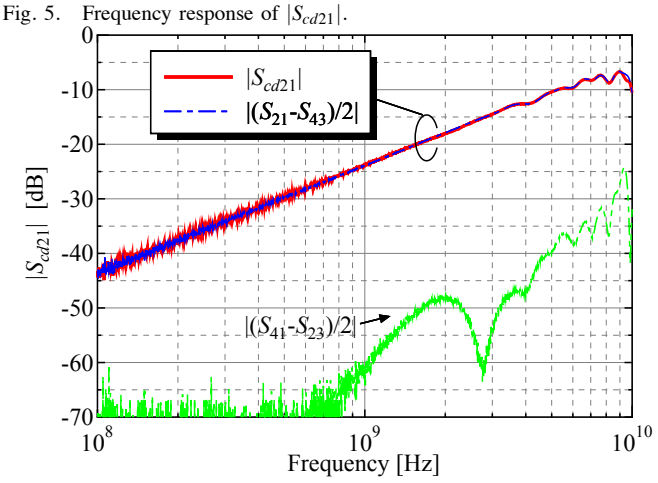

Fig. 6. Identification of dominant imbalance component in the "Weak-coupling" case.

The measured frequency responses of single-end *s*-parameter are shown in Fig. 6. Figure 6 clearly demonstrates that the dominant factor of generation of imbalance component of the model under study is difference of the transmission path due to the asymmetrical geometry. Consequently, since the dominant factor of generation of imbalance component of the model under study is difference of the geometrical length between

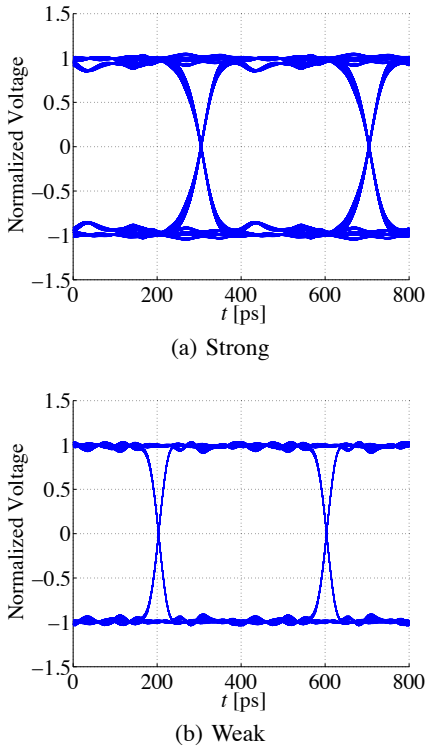

Fig. 7. Simulated differential-voltage V_{DS} (Eye-diagram) for 2.5 GHz input rectangular signal.

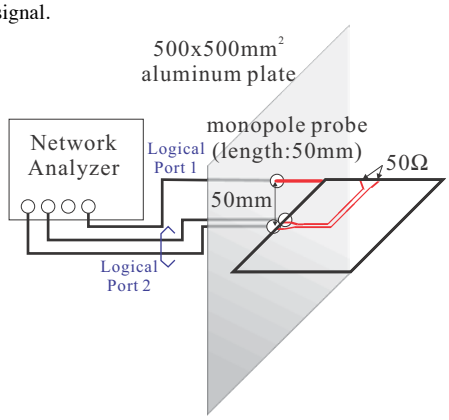

Fig. 8. Experimental setup for electric field near the PCB.

Line 1 and 2 due to the bend routing, the frequency response of imbalance component $S_{cd21}|$ up to 8 GHz follows 6 dB/octave (20 dB/decade).

Figure 7 shows the simulated eye-diagram for the differential-voltage, V_{DS}, for the 2.5 GHz ideal rectangular signal. As demonstrated in the frequency response of S_{dd21}, the "Weak" coupling is suitable for the improvement of signal integrity issues such as the eye-diagrams of high-speed digital circuits.

IV. Evaluation of Electric Field near a PCB

Frequency response of electric field near a PCB are discussed, from view point of EMI. A monopole probe with 50 mm length [12] and network analyzer were used to measure the electric field near the PCB, as shown in Fig. 8. The distance

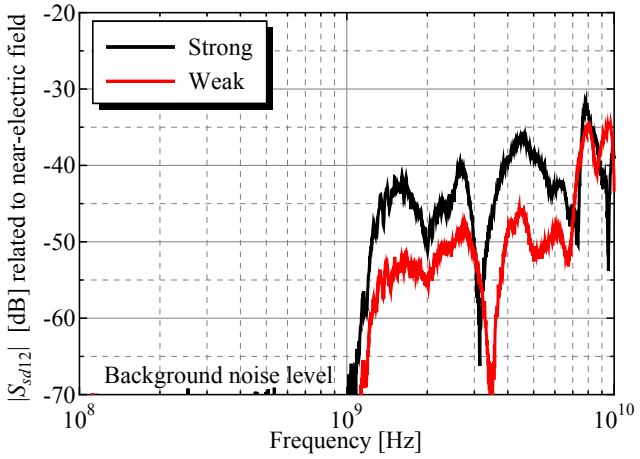

Fig. 9. Frequency response of $|S_{sd12}|$ related to electric-field (DM excitation).

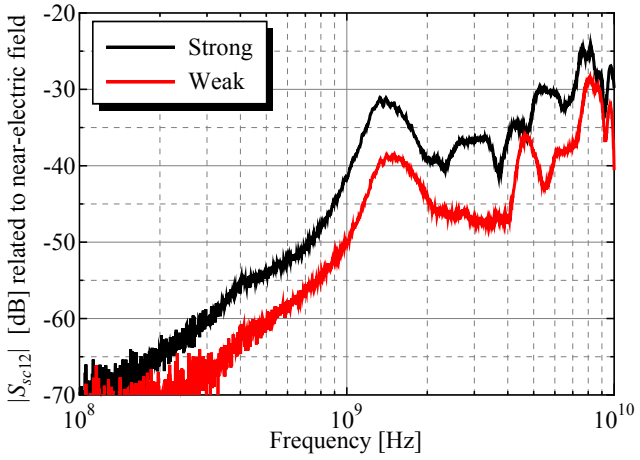

Fig. 10. Frequency response of $|S_{sc12}|$ related to electric-field (CM excitation).

between the monopole probe and the PCB is 50 mm. The $|S_{sd12}|$ and $|S_{sc12}|$ are related to the electric field near a PCB when the paired-lines are driven by DM and CM, respectively.

Figures 9 and 10 show measured frequency responses of $|S_{sd12}|$ and $|S_{sc12}|$, respectively. The $|S_{sd12}|$ and $|S_{sc12}|$ in the "Weak" case are small compared with the electric-field in the "Strong" cases. The reason is dense of electric-field between trace and ground plane, as well as suppression of $|S_{cd21}|$. The $|S_{sc12}|$ is much higher than $|S_{sd12}|$. The difference of magnitude between $|S_{sc12}|$ and $|S_{sd12}|$ is key parameter for evaluating the effectiveness of radiation improvement by the differential signaling. In the cases, the effectiveness of radiation improvement below 1 GHz is more than 30 dB. However, as frequency becomes higher, the effectiveness of radiation improvement is deteriorated (SE above 2 GHz is below 10 dB anymore).

V. Conclusions

In order to provide basic considerations for the realization of methods for predicting and suppressing the EM radiation from asymmetrical differential-paired lines, the imbalance component and EMI from strong and weak coupled differential-paired lines with bend discontinuities were studied experimentally and with modeling. It is demonstrated that the differential-paired line with weak-coupling is suitable for improving the SI performance and suppressing the EMI. In addition, the weak-coupling may by used for design of a meander delay line for high-density packaging, without the coupling between each trace. This study has successfully reported the basic characteristics of imbalance component of differential-paired lines with bend routing and demonstrates the dominant factor of imbalance component. Additionaly, the results can be used to development of design guidelines for both SI and EMI performances.

The clarification by transmission line approach to generation of imbalance component and the identifying the dominant radiation factor using the physics-based model are the future subjects for mitigating SI and EMI, developing guidelines in high-speed electronic designs.

Acknowledgment

The authors sincerely thank to Akita Industrial Technology Center, for their support of measurements.

References

[1] S. Hall, G.W. Hall, and J.A. McCall, *High-Speed Digital System Design: A Handbook of Interconnect Theory and Design Practices*, John Wiley & Sons, INC., New York, 2000.

[2] H. Johnson and M. Graham, *High-Speed Signal Propagation*, Prentice Hall PTR, 2003.

[3] A.C. Scogna and F. Zanella, "Broadband Signal Integrity Characterization of a High Speed Differential Backplane Pair", in *Proc. IEEE Int. Symp. Electromagn. Compat.*, pp.24–28, Portland, OR, Aug. 2006.

[4] T.L. Wu, Y.H. Lin, T.K. Wang , C.C. Wang and S.T. Chen, "Electromagnetic Bandgap Power/Ground Planes for Wideband Suppression of Ground Bounce Noise and Radiated Emission in High-Speed Circuits", *IEEE Trans. Microw. Theory Techn.*, vol.53, no.9, pp.2935–2942, Sep. 2005.

[5] G.H. Shiue, W.D. Guo, C.M. Lin and R.B. Wu, "Noise Reduction Using Compensation Capacitance for Bend Discontinuities of Differential Transmission Lines", *IEEE Trans. Adv. Packag.*, vol.29, no.3, pp.560–569, Aug. 2006.

[6] C. Gazda, D.V. Ginste, H. Rogier, R.B. Wu and D.D. Zutter, "A Wideband Common-Mode Suppression Filter for Bend Discontinuties in Differential Signaling Using Tightly Coupled Microstrips", *IEEE Trans. Adv. Packag.*, vol.33, no.4, pp.969–978, Nov. 2010.

[7] G.H. Shiue, J.H. Shiu, Y.C. Tsai and C.M. Hsu, "Analysis of Common-Mode Noise for Weakly Coupled Differential Serpentine Delay Microstrip Line in High-Speed Digital Circuits", *IEEE Trans. Electromagn. Compat.*, vol.54, no.3, pp.655–666, Jun. 2012.

[8] C.H. Chang, R.Y. Fang and C.L. Wang, "Bended Differential Transmission Line Using Compensation Inductance for Common-Mode Noise Suppression", *IEEE Trans. Compon. Packag. Manuf. Technol.*, vol.2, no.9, pp.1518–1525, Sep. 2012.

[9] Y. Kayano and H. Inoue, "Identifying EM Radiation from a Printed-Circuit Board Driven by Differential-Signaling", *Trans. JIEP*, vol.3, no.1, pp.24–30, Dec. 2010.

[10] Y. Kayano, K Mimura and H. Inoue, "Evaluation of Imbalance Component and EM Radiation Generated by an Asymmetrical Differential-Paired Lines Structure", *Trans. JIEP*, vol.4, no.1, pp.6–16, Dec. 2011.

[11] Y. Kayano, Y. Tsuda and H. Inoue, "Identifying EM Radiation from Asymmetrical Differential-Paired Lines with Equi-Distance Routing", in *Proc. IEEE Int. Symp. Electromagn. Compat.*, pp.311–316, Pittsburgh, PA, USA, Aug. 2012.

[12] Y. Kayano and H. Inoue, "Identifying Imbalance Component and EM radiation from Asymmetrical Differential-Paired Lines with Different U-Shape Bend Equi-Distance Routing", in *Proc. Pan-Pacific EMC Joint Meeting'12*, pp.195–198, Tokyo, Japan, Nov. 2012.

[13] Y. Kayano and H. Inoue, "Imbalance Component and EM Radiation from Differential-Paired Lines with Serpentine Equi-Distance Routing", in *Proc. IEEE Int. Symp. Electromagn. Compat.*, pp.359–364, Denver, CO, USA, Aug. 2013.